Questions Raised by Gas-Cavern Thermodynamics

Salt Production

Keywords: Cavern Thermodynamics

Abstract

Several topics related to gas-temperature changes in a gas-storage cavern are considered. Onset of thermal convection is discussed. A simple equation for temperature evolution is proposed, along with an approximate solution, valid for rapid injections or withdrawals. Good agreement was found with the results of an in-situ test performed by Crossley (1996). Influence of the radiation condition at the cavern wall proves to be relatively small.

Introduction

Gas-storage caverns used to be developed mainly for seasonal storage. Pressure changes were slow, and temperature changes were small. However, the needs of energy traders are prompting change toward more aggressive operating modes. At the same time, Compressed Air Energy Storages (CAES) are designed to deliver full-power capacity in a very short period of time. In such modes, temperature changes are much larger. This paper discusses some aspects of this issue.

Gas temperature in a cavern — Three examples

Klafki et al. (2003) discussed the case of a gas-filled cavern (Figure 1). At rest (Curve 1), the temperature gradient in the cavern ($G = dT/dz$, z oriented downward) is much smaller than the geothermal gradient, except at the bottom of the cavern, where a small amount of cold brine was left at the end of the first gas filling. After gas withdrawal, gas temperature drops but remains almost uniform, at least in the cavern main body (Curve 2).

However, at the Huntorf CAES, a few months after it was commissioned (Quast, 1993), the temperature gradient remained negative, even after several injection/withdrawal cycles (Figure 2). In the Enterprise natural gas cavern (Figure 3, Skaug et al., 2010), the temperature gradient is negative in the lower part of the cavern. Temperature drops after a significant withdrawal; however, temperature is almost uniform above the brine left at the cavern bottom.

berest@lms.polytechnique.fr +33 169 335 477

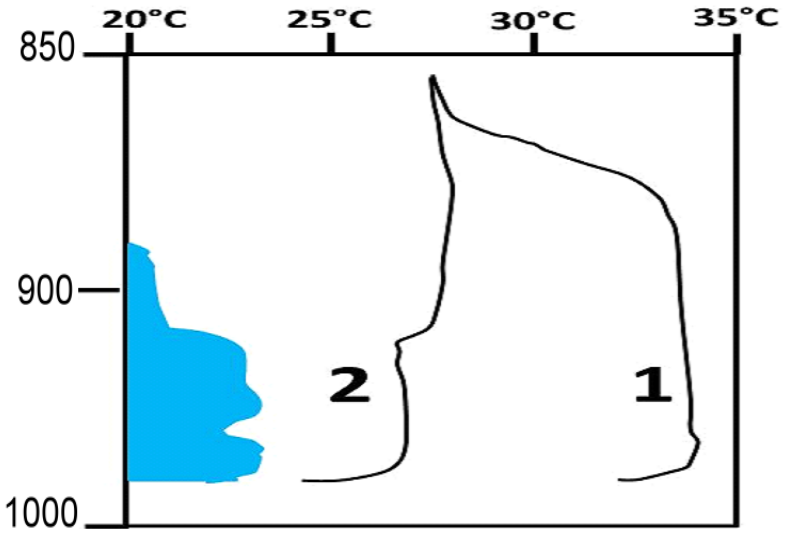

Figure 1. Cavern contour (left) is represented together with temperature profiles (1) at equilibrium and (2) after three consecutive withdrawals (after Klafki et al., 2003).

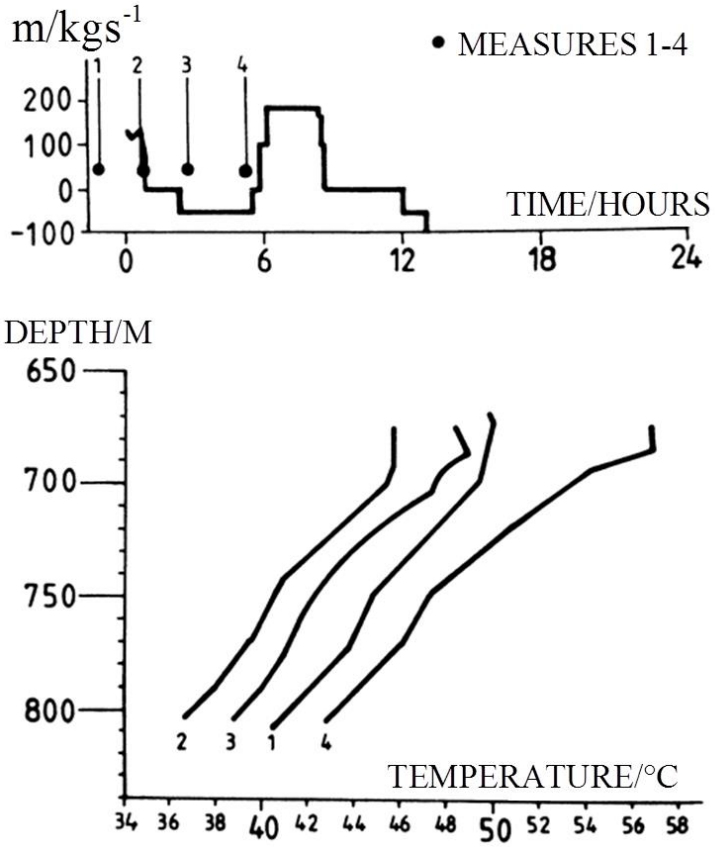

Figure 2. Gas flowrate (above) and temperature profiles in the Huntorf caverns (below) (after Quast, 1993).

berest@lms.polytechnique.fr +33 169 335 477

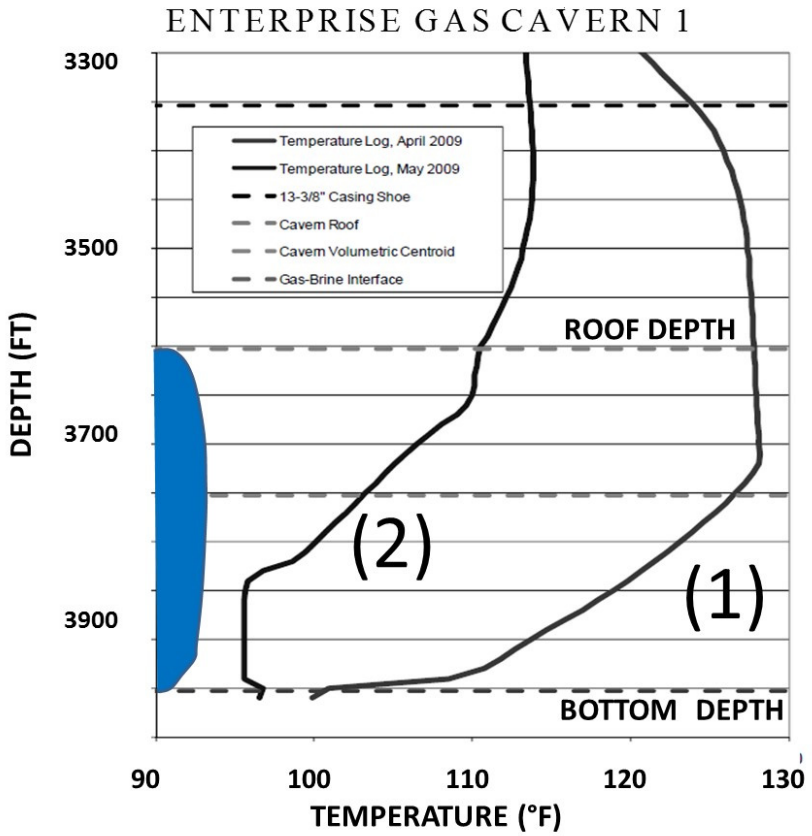

Figure 3. Temperature profiles in Enterprise Gas Cavern 1 (after Skaug et al., 2010).

Onset of thermal convection

In a rock mass, temperature is an increasing function of depth. In a salt formation, because salt thermal conductivity is larger than average rock conductivity ($K_{salt} = 6$ W/m-°C instead of $K = 3$ W/m-°C), the geothermal gradient is small; $G_{geo} = 1.5$ to 1.8°C/100 m is typical. Assume, first, that gas remains still in the cavern ($\mathrm{grad}P = \rho(P,T)g$), from which it can be inferred that $P = P(z)$ and $T = T(z)$.

Temperature distribution is harmonic (i.e., $\Delta T = 0$) both in the rock mass and in the cavern. In the cavern, the thermal gradient, or G_{eq}, is constant and, as gas is much less conductive than the rock mass, it is larger than the geothermal gradient. For instance, in an idealized spherical cavern, the thermal gradient is $G_{eq} = 3G_{geo}K_{salt}/(K_{gas} + 2K_{salt}) \approx 3G_{geo}/2$. The question is whether such equilibrium is stable.

Consider, first, the case of a dry gas. When a particle rises by $dz < 0$, its pressure decreases almost immediately by $dP = \rho g dz$ to reach mechanical equilibrium with surrounding gas. It cools

berest@lms.polytechnique.fr +33 169 335 477

accordingly; however, thermal equilibrium is slower to reach, as heat must be exchanged with the surrounding gas. The worst case is met when gas evolution is adiabatic (no heat exchange): $dP/P + \gamma dv/v = 0$, $\gamma = C_P/C_v$ and $G_{ad} = dT/dz = g/C_P$ (dry adiabatic gradient). C_p is the heat capacity when gas pressure is kept constant and $\gamma = C_p/C_v$ when the gas is perfect. When $G_{ad} = g/C_P < G_{eq}$, the particle at $z + dz$ is warmer and then lighter than the surrounding gas, and the particle keeps rising: convection cells appear, gas is stirred and the temperature gradient is small, as observed in Figure 1. For brine, $C_P = 3800$ J/kg-°C and $G_{ad} = 0.25$°C/100 m; $C_P = 2345$ J/kg-°C and $G_{ad} = 0.4$°C/100 m for natural gas; and $C_P = 1000$ J/kg-°C and $G_{ad} = 1°\mathrm{C}/100\ \mathrm{m}$ for air. Even for air, $G_{ad} = g/C_P < G_{eq}$, and, in principle, onset of convection is certain.

In fact, as some brine is left at cavern bottom during debrining, the cavern gas is saturated with water vapor, the temperature drop leads to condensation and, in principle, the “wet” adiabatic gradients should be considered. However, the ratio between wet and dry gradients is proportional to the ratio between partial water pressure and gas pressure; in a cavern, this ratio is exceedingly small.

However, immediately after leaching is completed, the brine is significantly colder than the rock mass at cavern-bottom depth. Such a cold source hinders the onset of convection (see the Huntorf case, Figure 2). Activity in the Entreprise Gas Cavern 1 (Figure 3) is more complex. At rest (Curve 1), gas is significantly warmer than bottom brine, and the thermal gradient is negative. (convection takes place in the brine.) After a significant gas withdrawal (Curve 2), gas is colder than brine at the bottom of the cavern, and thermal convection appears in the lower part of the cavern.

Temperature changes during gas withdrawal or injection

Energy balance equation

In this discussion, the thermodynamics of gas injection or withdrawal, it is assumed that gas temperature and pressure are uniform throughout the whole cavern. The first principle of thermodynamics (energy balance) can be written as

$$m\dot{h} = v\dot{P} + Q + <\dot{m}>\left(h^{inj} - h\right) \qquad (1)$$

where m is the gas mass [$<\dot{m}> = \dot{m}$ when gas is injected, $\dot{m} > 0$, and $<\dot{m}> = 0$ when gas is withdrawn, $\dot{m} < 0$], $h = h(P,T)$ is the gas enthalpy, and Q the heat flux from the rock mass. When gas is injected ($<\dot{m}> = \dot{m}$), gas pressure is continuous at the cavern neck, but gas temperature is not, and an jump in enthalpy must be considered at the cavern entrance $\left(h^{inj} - h = C_P\left(T^{inj} - T\right)\right)$: $h = C_P T$ and $Pv = rT$. In addition, during gas movement, the elastic cavern-volume change can be neglected, $mv = V_0$. The thermal diffusivity of salt is $k_{salt} = 3\times10^{-6}\ \mathrm{m}^2/\mathrm{s}$, and only fast injection

berest@lms.polytechnique.fr +33 169 335 477

and withdrawal are considered. The depth of penetration of gas-temperature changes in the rock mass after a time Δt is approximately $\sqrt{k_{salt}\Delta t}$, or $\sqrt{k_{salt}\Delta t} = 1\,\text{m}$ when $\Delta t = 4$ days. In other words, at such a time scale, the cavern surface can be considered as the sum of small flat surfaces whose total area equals the actual area of the cavern walls (Σ), as was noted by Crotogino et al. (2001) and Krieter (2011).

At the cavern wall, two types of boundary conditions generally are considered. The simpler consists of assuming that temperature is continuous:

$$T_{wall} = T \tag{2}$$

The second consists of assuming that there is a temperature jump at the cavern wall and that this jump is proportional to the heat flux crossing the wall (Newton's condition). This last approximation accounts for the development of a boundary layer at the cavern wall whose thickness is a function of wall roughness and the development of a gas tangential rate at the cavern wall:

$$\frac{\partial T_{wall}}{\partial n} = H\left(T_{wall} - T\right) \tag{3}$$

where n is the outward normal-unit vector, see for instance, Kushnir et al., 2012. However, the exact value of H is little-known (and even not specified in many papers). When (2) applies, the energy equation (1) can be written

$$\left(\frac{\gamma}{\gamma-1}\right)\frac{P\dot{T}}{T} - \dot{P} = -\frac{\Sigma K_{salt}}{V_0}\int_0^t \dot{T}_{wall}(\tau)\Big/\sqrt{\pi k_{salt}(t-\tau)}\,d\tau \qquad (withdrawal,\ \dot{m} < 0) \tag{4}$$

$$\frac{d}{dt}\left[\frac{P}{\gamma-1}\left(1-\frac{\gamma T^{inj}}{T}\right)\right] = -\frac{\Sigma K_{salt}}{V_0}\int_0^t \dot{T}_{wall}(\tau)\Big/\sqrt{\pi k(t-\tau)}\,d\tau \qquad (injection,\ \dot{m} > 0) \tag{5}$$

When (3) is considered instead of (2):

$$\frac{\gamma}{\gamma-1}\frac{P\dot{T}}{T} - \dot{P} = -\frac{\Sigma H}{V_0}\int_0^t \exp\left[h^2 k_{salt}(t-\tau)\right] erfc\left[h\sqrt{k_{salt}(t-\tau)}\right]\dot{T}_{wall}(\tau)\,d\tau \tag{6}$$

where $h = H/K$. The evolution is adiabatic when $H = 0$ and (6) coincides with (4) when $H = \infty$.

A closed-form solution

Computing a numerical solution for (3) and (4) using a small computer is easy. The accuracy of the numerical procedure can be assessed using the following closed-form solution of (3) and (4):

$$P(t) = -\pi\frac{K_{salt}}{\sqrt{\pi k_{salt}}}\frac{2\gamma}{4(\gamma+5)}t^3 \qquad T(t) = \frac{4}{15}t^{5/2}.$$

berest@lms.polytechnique.fr +33 169 335 477

A simplified solution

When Eq. (2) is accepted, a simplified solution of Eq. (3) can be reached. Initial pressure and temperature are P_0 and T_0, respectively. It is assumed that temperature decreases by a small amount ($\Delta T < 0$) during a Δt-long period and that temperature rate is constant; $\Delta T/T$ is close to $\Delta T/T_0$. Then, Eq. (2) can be solved as follows:

$$\frac{\Delta P}{\Delta T} = \left(\frac{4}{3} \frac{\Sigma}{V} \frac{K_{salt}}{\sqrt{\pi k_{salt}}} \sqrt{\Delta t} + \frac{\gamma}{\gamma - 1} \frac{P_0}{T_0} \right) \tag{7}$$

This simple formula allows assessing the respective parts played by gas expansion and heat flow. The value of the gas constant is $\gamma = 1.4$ (air, hydrogen) or $\gamma = 1.3$ (methane). The influence of the thermal properties of rock is through the parameter $K_{salt}/\sqrt{\pi k_{salt}}$, whose value typically is $K_{salt}/\sqrt{\pi k_{salt}} = 1800$ W.s$^{1/2}$-m^2 (see Table 1). Initial temperature T_0 belongs to the range 300-330 K. Equation (7) proves that the temperature drop (for a given pressure drop) is larger when the initial pressure, P_0, is smaller, as was noted by Zapf et al. (2015). When the depressurization time is shorter, as expected; when the ratio V/Σ is smaller. Staudtmeister et al. (2011) suggest $V/\Sigma = 8 - 12$ m. Rokahr et al. (2011) mention that "*the ratio V/Σ is usually less than 10 m for caverns in salt domes because they are often shaped long and thin*" (p. 194). In an idealized spherical cavern with radius *a*, for instance, V = 525,000 m^3, $a = 50$ m, and $V/\Sigma = a/3 = 17$ m.

	K_{salt} (W/m/°C)	ρ (kg/m^3)	C_p (J/kg/°C)	k_{salt} (m^2/s)	$K/\sqrt{\pi k}$ (SI)
Pellizzaro et al., 2011	5.2	2174	800	2.99×10^{-6}	1700
Staudtmeister et al., 2011	5.5	2180	870	2.9×10^{-6}	1820
Blanco Martin et al.	5	2200	860	2.64×10^{-6}	1740
LOCAS	6.1	2200	921	3×10^{-6}	1980

Table 1: Thermal parameters.

Consider the case of a CAES cavern where $C_p = 1005.2$ J/kg-°C, $C_v = 718.5$ J/kg-°C, $K_{salt}/\sqrt{\pi k_{salt}} = 1980$ W.s$^{1/2}$-m^2, and $T_0 = 308.5$ K. Depressurization lasting one day will lead to

$$\Delta P/\Delta T \left[in \text{ MPa/°C} \right] = 0.78 \ \Sigma/V \left[\text{m}^{-1} \right] + 0.011 \ P_0 \left[\text{MPa} \right] \tag{8}$$

Several cases are considered in Table 2. The adiabatic case $(V/\Sigma = \infty)$ is provided for comparison. Numerical computations can provide a more precise picture of temperature evolution when longer time periods are considered. When performing accurate numerical computations,

berest@lms.polytechnique.fr +33 169 335 477

especially in a CAES, the mesh size at the cavern wall must be small. (For example, Pellizzaro et al. (2011) and Brouard et al. (2011) suggest 30 cm and 10 cm, respectively.) The last column of Table 2 provides the results of numerical computations performed with the LOCAS software; they are compared to the results provided by Eq. (3), which provides an acceptable approximation.

$\gamma/(\gamma-1)$	P_0 **(MPa)**	V/Σ **(m)**	Δt **(day)**	$\Delta T/\Delta P$ **(°C/MPa)**	**LOCAS**
3.548 (air)	12	11.5	1	4.87	4.7
4.378 (CH_4)	12	11.5	1	4.22	4.4
3.548 (air)	6	11.5	1	6.58	7.05
3.548 (air)	12	22.5	1	5.78	5.9
3.548 (air)	12	11.5	4	3.67	3.61
3.548 (air)	12	∞	0	7.25	

Table 2: Temperature drop (ΔT) following a δt-long pressure drop by ΔP = 1 MPa.

Testing in a Melville Cavern (Crossley, 1996)

Equations (2) and (4) were validated against the results of a withdrawal test described by Crossley (1996) and performed in the Regina #5 gas-storage cavern in Melville, Canada. The volume of this cavern is $V = 46{,}000$ m^3. The flow rate and gas-temperature evolution as measured during the test are represented on Figure 3. Gas was withdrawn over 18 days. The following values were selected: $\gamma = 1.305$ and $\Sigma = 12{,}415$ m^2. (Other values also were considered, but they did not provide a better fit.) Results of the computations are provided on Figure 4. Good agreement between computed and measured temperatures is met. Note that slightly before the end of the withdrawal phase (day 5), gas begins to warm, due to the high heat flux from the rock mass. Figure 4 also displays the computed evolutions when the radiation condition (3) is taken into account; various values of $h = H/K$ were selected. Differences are relatively small.

Conclusion

During fast injections and withdrawals, gas temperature in a storage cavern experiences large changes. A relatively simple model allows computing temperature evolution accurately and proves that a small number of parameters play a significant role.

berest@lms.polytechnique.fr +33 169 335 477

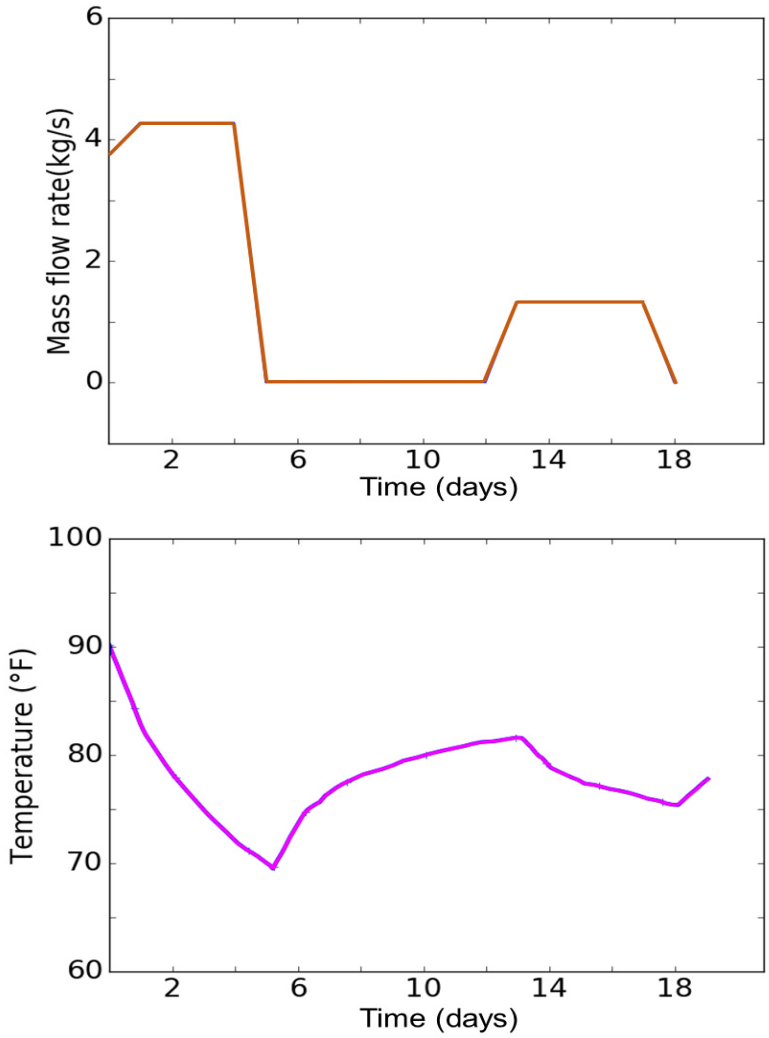

Figure 3. Gas withdrawal rate and temperature evolutions (after Crossley, 1996).

berest@lms.polytechnique.fr +33 169 335 477

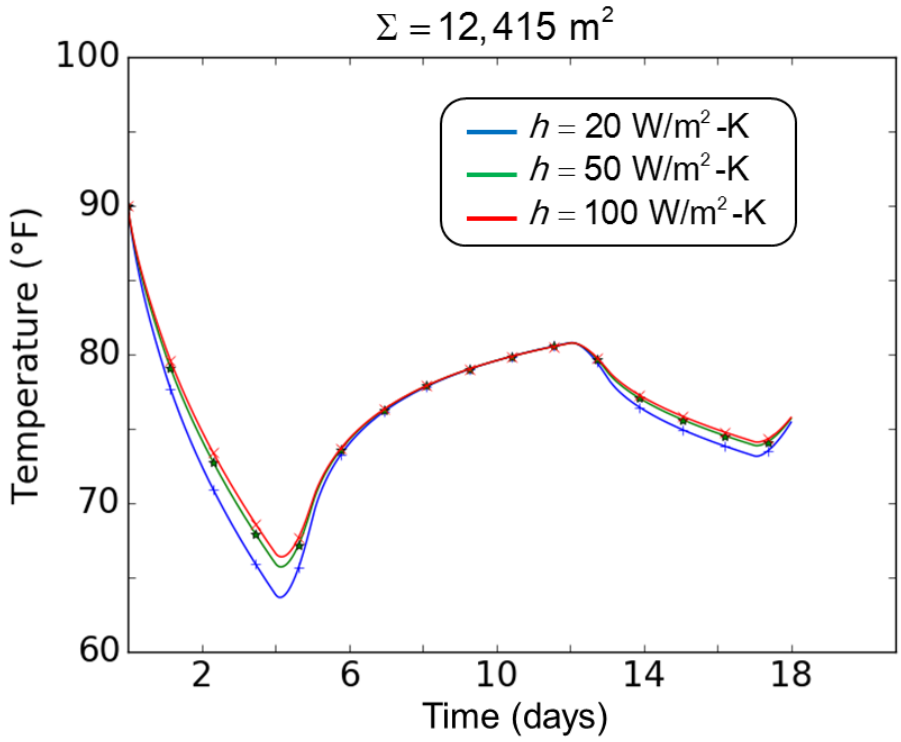

Figure 4. Computed temperature evolution and influence of the radiation condition.

References

Brouard B., Frangi A. and Bérest P. (2011). Mechanical stability of a cavern submitted to high-frequency cycles. In *Proc. SMRI Spring Meeting, Galveston, Texas*, 99-116.

Crossley N.G (1996). Salt cavern Integrity Evaluation Using Downhole Probes. A Transgas Perspective. SMRI Fall Meeting, Cleveland, Ohio, 21-54.

Crotogino F., Mohmeyer K.U. and Scharf R. (2001). Huntorf CAES: More than 20 years of successful operation. In *Proc. SMRI Spring Technical Conferenc*e, Orlando, Florida, 351-362.

Klafki M., Wagler T., Grosswig S. and Kneer A. (2003). Long-term downhole fibre optic temperature measurements and CFD modeling for investigation of different gas operating modes. SMRI Fall Meeting, Chester, UK, 180-189.

Krieter M. (2011). Influence of gas cavern's surface area on thermodynamic behaviour and operation. In *Proc. SMRI Fall Meeting, York, UK,* 179-184.

Kushnir R., Dayan A. and Ullmann A. (2012). Temperature and pressure variations within compressed air energy storage caverns. *Int. J. Heat and Mass Transfer.* 55: 5616-5630.

Pellizzaro C., Bergeret G., Leadbetter A. and Charnavel Y. (2011). Thermomechanical behavior of Stublach gas storage caverns. In *Proc. SMRI Fall Meeting, York, UK*, 161-178.

berest@lms.polytechnique.fr +33 169 335 477

Quast P. (1993). L'installation de Huntorf : plus de trois années de fonctionnement de cavernes à air comprimé. Annales des Mines, 190ème année, n°5-6, mai-juin 1983, 93-102.

Rokahr R., Staudtmeister K. and Zapf D. (2011). Rock mechanical design for a planned gas cavern field in the Preesall Project Area, Lancashire, UK. In *Proc. SMRI Fall Meeting, York, UK,* 189-204.

Skaug N., Ratigan J. and Thompson M. (2010). Natural Gas Cavern Inventory assessment — A New approach. In *Proc.* SMRI Spring Meeting, Grand Junction, Colorado, 303-312.

Staudtmeister K., Zapf D. and Leuger B. (2011). The influence of different loading scenarios on the thermo-mechanical behavior of a gas storage cavern. In *Proc. SMRI Spring Meeting, Galveston Texas*, 83-97.

Zapf D., Staudtmeister K., Rokahr R.B., Yildirin S., Leuger B., Donadei S., Zander-Schiebenhöfer D., Horvath P.L., Fleig S., Pollok L. and Hölzner M. (2015). Salt structure information system (InSpEE) as a supporting tool for evaluation of storage capacity of caverns for renewable energies/rock mechanical design for CAES and H_2 storage caverns. In *Proc. Mech. Beh. Salt VIII,* 291-297. London: Taylor & Francis Group.

berest@lms.polytechnique.fr +33 169 335 477